Environmental and
Biogeochemical Processes

Original Research

Open Access

https://doi.org/10.48130/ebp-0025-0007

Patterns and drivers of soil denitrification and its responses to nitrogen addition in steppe ecosystems

Dan Yuan[1#], Xiaodong He[2#], Tim J. Clough[3], Chunsheng Hu[1], Xiangzhen Li[4], Minjie Yao[4] and Shuping Qin[1*]

Received: 27 June 2025

Revised: 14 August 2025

Accepted: 8 September 2025

Published online: 21 October 2025

Abstract

Soil denitrification, a pivotal microbial process responsible for ecosystem nitrogen loss and the emission of the greenhouse gas nitrous oxide (N_2O), is intricately influenced by climate conditions and inherent soil properties. Despite the importance of denitrification, there is a lack of information regarding the dominant environmental factors driving denitrification rates in steppe ecosystems, especially at regional and sub-regional geographical scales. The Eurasian steppe is the largest steppe region in the world and is a crucial component of the global grassland ecosystem. To address this gap, a comprehensive examination was conducted across three regions of the Eurasian steppe: the Loess Plateau (LP), the Inner Mongolian Plateau (IMP), and the Xizang Plateau (XP). The denitrification potential (encompassing N_2O and N_2 emissions) of sampled soils was evaluated. This denitrification potential was delineated based on regional and sub-regional attributes. While total nitrogen (TN) was the overarching determinant of denitrification potential at the regional scale, a more granular assessment revealed soil total carbon (TC), mean annual precipitation (MAP), and TN as pivotal contributors to the observed variance in denitrification potential across the steppe regions. Notably, N addition directly significantly regulates N_2O emissions, a key component of denitrification potential across all sampling sites. This study enhances our understanding of factors governing denitrification potential and, consequently, N_2O emissions in steppe soils: as the world experiences climatic shifts characterized by warming and increased humidity, these insights assume heightened relevance. The results indicate that steppes are poised to amplify denitrification processes and consequential N_2O emissions. Importantly, as nitrogen deposition increases globally, regions with intrinsic nitrogen sensitivities, exemplified by areas like the XP, may experience a disproportionate surge in N_2O emissions. This underscores the pressing need for targeted interventions and mitigation strategies in such vulnerable regions.

Keywords: N_2O emission, $N_2O/(N_2O + N_2)$, Environmental factor, Chinese steppe, PLS path modeling

Highlights

- TN is the primary regional-scale driver of denitrification potential.
- TC, MAP, and TN collectively explain the variance in denitrification rates at the sub-regional level.
- N addition directly regulates denitrification potential across all sampling sites.

Authors contributed equally: Dan Yuan and Xiaodong He

* Correspondence: Shuping Qin (qinshuping@sjziam.ac.cn)

Full list of author information is available at the end of the article.

Graphical abstract

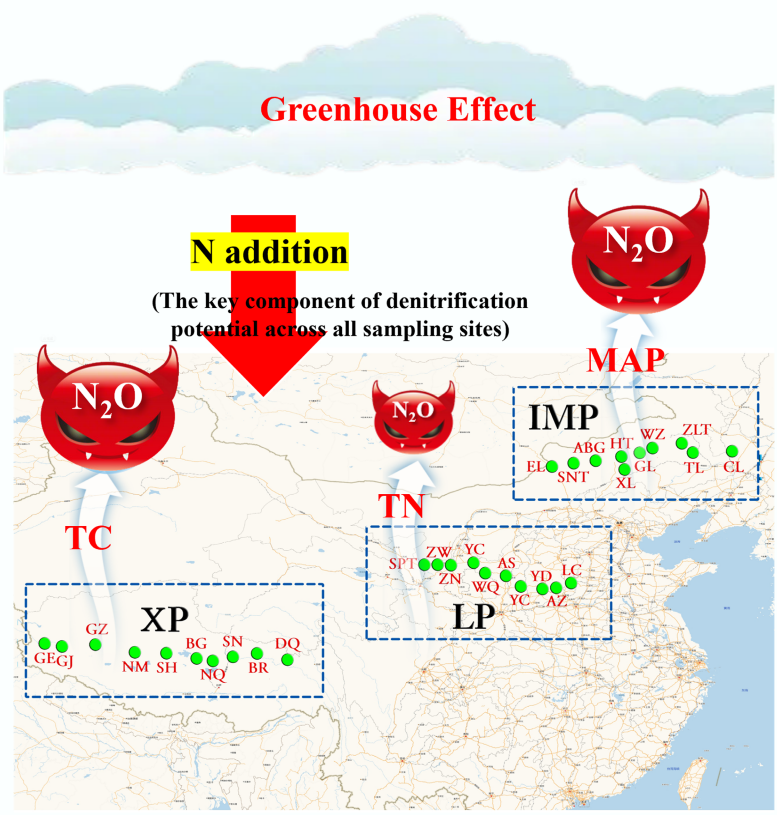

Notes: TC, TN and MAP was the driver of N_2O emissions at XP, LP and IMP steppe, respectively. TC: total carbon; TN: total nitrogen; MAP: mean annual precipitation.

Introduction

Nitrous oxide (N_2O) is a long-lived greenhouse gas that has a global warming potential of 298 times greater than that of CO_2 over a 100-year period[1,2], and is the primary contributor to stratospheric ozone depletion[2]. Atmospheric concentrations of N_2O have increased since pre-industrial times due to anthropogenic activities, with terrestrial ecosystems serving as the primary source of N_2O emissions, derived via denitrification[3,4].

Grasslands comprise approximately 20% of the Earth's terrestrial surface[5,6]. The Eurasian steppe is the largest steppe region in the world, covering an area of about 150 million hectares, and is an important part of the global grassland ecosystem. The North Chinese steppes are located in the central part of the Eurasian steppe, include the Loess Plateau (LP) steppe, the Inner Mongolian Plateau (IMP) steppe, and the Xizang Plateau (XP) steppe. The estimated total annual N_2O emissions from temperate grassland ecosystems in China amount to 112.13 Gg N yr^{-1}[7]. Nitrous oxide emissions derived from soil denitrification are a significant contributor to global N_2O emissions, and these emissions may, in turn, be affected by changes in climate.

Previous research on denitrification rates within grassland soils has mostly focused on N_2O emissions influenced by grazing, climatic factors, microorganisms, and fertilization[8–11]. Grazing has been shown to increase total N_2O emissions by up to 68%, relative to ungrazed soil[10]. On the contrary, Zhong et al.[12] found that as grazing intensity increased, there was a significant reduction in the potential rate of denitrification. Fluxes of N_2O from grassland steppe soils have been shown to be positively correlated with soil water-filled pore space (WFPS), soil temperature, dissolved organic carbon (DOC), and soil NO_3^-–N concentration[11,13]. Moreover, grassland steppe soil denitrification potentials were able to be explained by microbial factors, like *nirS* gene expression level, and nitrifier/denitrifier abundances[11]. The application of nitrogen fertilizers is a crucial management strategy in grassland ecosystems[14], and it contributes significantly to the denitrification rate[15]. In addition to the aforementioned factors, nitrogen input or deposition is also closely associated with denitrification potential in grassland soils. Based on the assessment in 2000, the N deposition rates in most parts of the world are greater than 10 kg N ha^{-1} yr^{-1}, and showed an increasing trend. By 2030, the rate of N deposition is projected to exceed 15 kg N ha^{-1} yr^{-1} in most areas of the world, including the Xizang Plateau steppe[16]. Geng et al.[17] demonstrated that the potential of denitrification in an alpine grassland steppe was significantly enhanced by high levels of nitrogen input (≥ 30 kg N ha^{-1} yr^{-1}).

Regional climate, including mean annual precipitation (MAP), and mean annual temperature (MAT), also significantly affects the N_2O emissions of grassland soil. A meta-analysis showed that annual N_2O fluxes ranged from −0.33 to 2.14 kg N_2O–N ha^{-1} yr^{-1}, of which their spatial distribution across ecosystems were mainly reflected by MAP and warming over the XP region[18]. The intra- and inter-annual variations in N_2O emissions were mainly triggered by temporal

dynamics of soil temperature and moisture conditions[19]. A soil laboratory experiment, sampled at the Inner Mongolia grasslands, revealed that N_2O fluxes were significantly correlated with soil temperature[20].

Global grasslands potentially contribute 30% of total N_2O flux to the atmosphere. N_2O mainly originates from microbial denitrification processes[21]. The end-product of denitrification is dinitrogen (N_2), which results from the reduction of soil N_2O. However, to date, most research on denitrification in steppe soils has focused solely on N_2O emissions and has not considered N_2 emissions. Currently, the majority of research on denitrification rates from steppe soils has been performed on the Inner Mongolian or Xizang Plateau soils. However, it is worth noting that there is heterogeneity in denitrification responses across different steppe types. Previous studies have found that the typical steppe may hold the lowest N_2O emission[22]. Thus, to gain a deeper understanding of the soil denitrification potential (N_2O and N_2 emissions) within steppe ecosystems, a mesocosm experiment was performed using soils taken from three sites within the Eurasian steppe: Xizang Plateau, Loess Plateau, and the Inner Mongolian Plateau. Environmental variables influencing denitrification potential were also investigated, taking into account the variations in geography, climate, and soil physicochemical properties among sampling sites. Additionally, the study examined nitrogen addition as a crucial factor affecting grassland soil denitrification potential.

Materials and methods

Study site description

The three steppe sites were located in China on the Loess Plateau (LP), the Inner Mongolia Plateau (IMP), and the Xizang Plateau (XP), respectively (Fig. 1). The LP steppe is situated in a climatic zone characterized by semi-aridity and semi-humidity[23]. The sampling site spans from 35.99° N to 37.58° N, and from 104.44° E to 113.36° E, with an elevation range of 804–1,714 m. Mean annual temperature (MAT) ranges from 7.7 to 11.3 °C, while mean annual precipitation (MAP) varies between 188 and 599 mm. The grassland types present include meadow grassland, typical grassland, and desert grassland. The main representative plants in this study area include *white grass*, *Lespedeza japonicum*, and *artemisia annua*. Soil types found in this steppe region include brown, black, and gray calcium soils, as based on the FAO classification system[24]. The IMP steppe is situated in a mid-temperate monsoon climate that is semi-arid and humid. The sampling site spans from 43.55° N to 45.11° N, and from 112.15° E to 123.51° E, with an extensive altitude range of 144 to 1,272 m. MAT varies between 1.0 and 6.7 °C, while MAP ranges from 183 to 425 mm. The grassland types encompass meadow grassland, typical grassland, and desert grassland, and the surface vegetation is mainly *reed* and *setaria ephedra*. The IMP soils are categorized as chernozem, chestnut, and brown soils, according to the FAO classification system[24]. The XP steppe is situated in a plateau mountain climate, with sampling sites ranging from 31.38° N to 32.48° N and between 80.15° E to 95.45° E at altitudes of 4,104 to 4,617 m. The MAT varies from −0.3 to 0.9 °C, while the MAP ranges from 75 to 606 mm annually. Grassland types include alpine meadow grassland, alpine grassland, and alpine desert grassland. Representative plants include *Stegwoet*, *Kobresia,* and *Mountain Velingia*. All soil types are classified as alpine soil according to the FAO system[24]. Sampling site locations are shown in Fig. 1.

Soil samples were collected from 10 sites in each steppe in the growing season from July to August 2018. Ten sampling sites that were not subject to human disturbance were set up in each transect. Each steppe area comprised three meadow regions, four typical regions, and three desert regions, totaling 30 sampling sites. These sites had minimal human or cattle disturbances: five plots were selected at each site, with a distance of 100 m between each site. In each 1 m × 1 m plot, a composite sample was created by pooling together five soil cores (10 cm deep and 5 cm in diameter). Thus, a total of 150 soil samples were collected from three steppes at 30 different sites. Soil samples were placed in sterile plastic bags, surrounded by ice packs, and transported to the laboratory as soon as possible. The soil samples were passed through a 2.0 mm mesh and subsequently stored at 4 °C for the determination of soil physiochemical properties, denitrification potential (N_2O and N_2 emissions), and nitrogen addition experiments.

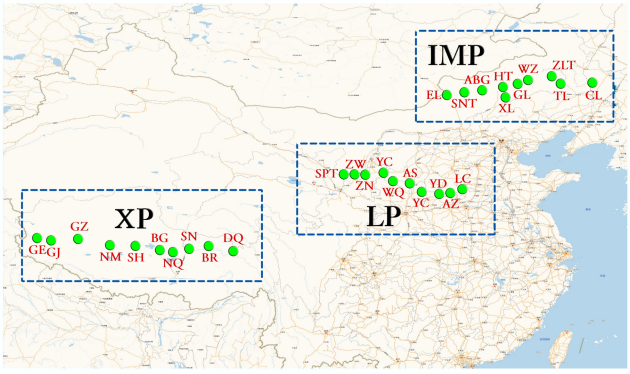

Fig. 1 Sampling sites distributed in LP, IMP, and TP steppe soils of China. The full site names of the abbreviated sample sites are listed in Table 1. LP, Loess Plateau; IMP, Inner Mongolia Plateau; XP, Xizang Plateau.

Measurement method

Soil nitrate (NO_3^-–N), nitrite (NO_2^-–N), ammonium (NH_4^+–N), and dissolved organic carbon (DOC) were extracted using 1 M KCl solution with a soil/water weight ratio of 1/5. The concentrations of NO_3^-–N, NO_2^-–N, and NH_4^+–N were determined by dual-wavelength spectrophotometry, the ethylenediamine dihydrochloride colorimetry method, and the indophenol blue colorimetry method, respectively[25–27]. The concentrations of DOC, dissolved inorganic carbon (DIC), and total inorganic carbon (TIC) were determined using a TOC analyzer (TOC-L CPH, Shimadzu, Japan). The water content was measured gravimetrically using the constant weight drying method.

Methods to determine the pH, electrical conductivity (EC), total nitrogen (TN), total phosphorus (TP), total potassium (TK), total carbon (TC), total organic carbon (TOC) of soil, MAT, and the MAP are described in detail by Xu et al.[24]. Briefly, soil pH was determined in a 1:2.5 (w/v) soil water suspension using the Ultrameter II 6PFCE (MYRON, USA). Soil TN was analyzed with an elemental analyzer (Elementar, Germany), while soil TP was quantified by ICP-OES (Optima 5300 DV, PerkinElmer, Waltham, MA, USA) after HNO_3 and HF digestion. Soil total organic matter was measured using the K_2CrO_7-H_2SO_4 oxidation method. MAT and MAP were obtained from the National Meteorological Information Center of China. Soil physicochemical properties are shown in Supplementary Table S1.

Microcosm experimental design

All soil samples, with and without added nitrogen source (NO_3^-–N, 10 kg N ha^{-1}, as KNO_3, approximately 1/10 of soil TN), and a water content of 20% (gravimetric), were placed into 120 ml flasks. Three biological replicates were prepared per treatment. The flasks were

sealed with air-tight butyl rubber septa and aluminum caps, then made anoxic by alternately evacuating (0.1 kPa), and filling with high-purity helium (99.999%, 120 kPa) five times. All flasks were incubated in a thermostat water bath at 25 °C for 168 h. The N_2O and N_2 concentrations in the headspace were measured using an automated system as previously described[28].

Statistical analyses

Spearman correlation was employed to examine the relationship between each influencing factor and the rates of N_2O and N_2 emission, and the $N_2O/(N_2O + N_2)$ ratio. The 'SoDA' package in R was utilized to transform the longitude and latitude into Cartesian coordinates. Subsequently, the 'Vegan' package (REF) was employed to convert these Cartesian coordinates into PCNM parameters, which were subsequently utilized as spatial variables. Using the 'PLSPM' package in R (REF), a partial least squares (PLS) path analysis was conducted to investigate the relationships between N_2O and N_2 production rates with geographical distance (PCNM, altitude), environmental parameters (soil physical and chemical properties: pH, TOC, TC, DOC, DC, C/N, TP, TK, BD, EC, TN, NO_3^-, NH_4^+, and NO_2^-; climatic factors: MAP and MAT), and nitrogen addition. Finally, a stepwise multiple linear regression analysis was conducted in R ('olsrr' package) to identify the optimal model for determining the primary factors influencing denitrification potential in the steppe soils.

Results

Soil denitrification potential

As shown in Fig. 2a, the N_2O emission rates varied between 0.6 ± 0.03 and 372.7 ± 32.5 μg N kg^{-1} dry soil h^{-1} across all 30 sampling sites. In the IMP steppe sites, N_2O emission rates varied from 2.4 ± 0.2 to 179.9 ± 14.8 μg N kg^{-1} dry soil h^{-1}, while for the LP steppe sites, they ranged from 3.2 ± 0.1 to 154.7 ± 20.3 μg N kg^{-1} dry soil h^{-1}. The mean N_2O emission rates in XP soils (61.0 μg N kg^{-1} dry soil h^{-1}), and IMP soils (60.9 μg N kg^{-1} dry soil h^{-1}) were significantly higher than those in LP soils (38.6 μg N kg^{-1} dry soil h^{-1}), indicating that XP and IMP are relative hotspots for N_2O emissions. The N_2 emission rates (Fig. 3a) ranged from 18.1 ± 2.7 to 1,230 ± 14.1 μg N kg^{-1} dry soil h^{-1} across all sampling sites. Consistent with the soil N_2O emission rates, the average level of soil N_2 emission rate in the XP sites (318.1 μg N kg^{-1} dry soil h^{-1}) was significantly higher than that of both the IMP (200.3 μg N kg^{-1} dry soil h^{-1}), and LP sites (142.5 μg N kg^{-1} dry soil h^{-1}). The $N_2O/(N_2O + N_2)$ ratio (Fig. 4a) exhibited a wide range of variation across all sampling sites, ranging from 0.7% to 73.8%. Specifically in LP sites, the $N_2O/(N_2O + N_2)$ rate ratios ranged from 3.4% to 73.8%, which were significantly higher than those observed in IMP sites (ranging from 1.5% to 42.3%) and XP sites (ranging from 0.7% to 44.7%).

Denitrification potential response to nitrogen addition

Nitrogen addition enhanced soil denitrification potential by 65%, on average, compared to the control (Fig. 2b). The mean N_2O emission rate across all 30 sampling sites with and without N-addition was 88.4 ± 14.6 and 53.5 ± 19.8 μg N kg^{-1} dry soil h^{-1}, respectively. At steppe scales, the average N_2O emission rates in the XP, IMP, and LP steppes were 121.3 ± 14.9, 101.3 ± 12.4, and 37.7 ± 5.6 μg N kg^{-1} dry soil h^{-1}, respectively. After nitrogen addition relative to the sampling sites without nitrogen addition, the mean N_2O emission rates increased by 98.8% and 66.3% in the XP and IMP steppes, respectively, while there was no significant effect on the mean N_2O emission rate in the LP steppe (Fig. 2a).

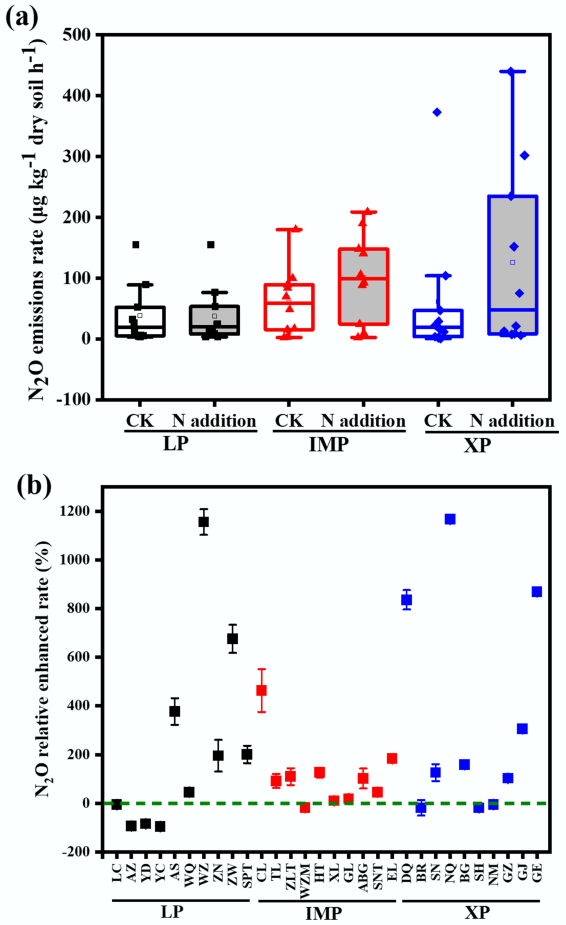

Fig. 2 (**a**) N_2O emission rates of steppe soils at different sites for the Loess Plateau (LP), Inner Mongolia Plateau (IMP), and Xizang Plateau (XP) steppes without and with N addition, and (**b**) the relative enhancement of emission rates after N addition, compared to the scenario without N addition. The concentration of N addition is 10 kg N ha^{-1}.

Addition of nitrogen also enhanced N_2 emission rates across most sampling sites, ranging from 59.2 ± 4.4 to 625.7 ± 194.8 μg N kg^{-1} dry soil h^{-1} (Fig. 3a) with an average 44.3% increment across all steppes (Fig. 3b). In the LP steppe sites, the soil N_2 emission rates increased by 185.9 μg N kg^{-1} dry soil h^{-1} (130.5%), while in the IMP steppe sites, N_2 emission rates increased by an average of 100.3 μg N kg^{-1} dry soil h^{-1} (50.1%). In XP steppe sites, the N_2 emission rates were less responsive to nitrogen addition, with an average increase of only 2.1%. Nitrogen addition altered the $N_2O/(N_2O + N_2)$ ratio. This ratio decreased by an average of 11.3% in the LP sites, but increased by an average of 5.0% and 6.1% in the IMP and TP sites, respectively (Fig. 4b).

Relationships between denitrification potential, environmental variables, and N addition

Spearman correlation analysis revealed that the relationship between environmental factors and denitrification potential varied between steppe and between sites within a steppe (Table 1). Combining data from all steppes, the denitrification potential for N_2O showed a positive correlation with MAP, TOC, TC, TN, DOC, NH_4^+–N, DN, and N-addition, and a negative correlation with MAT, pH, bulk density, DIC, and NO_2^-–N. In the LP steppe, the N_2O emission rates from sites were positively correlated with EC, C/N, NH_4^+–N, and N-addition, while

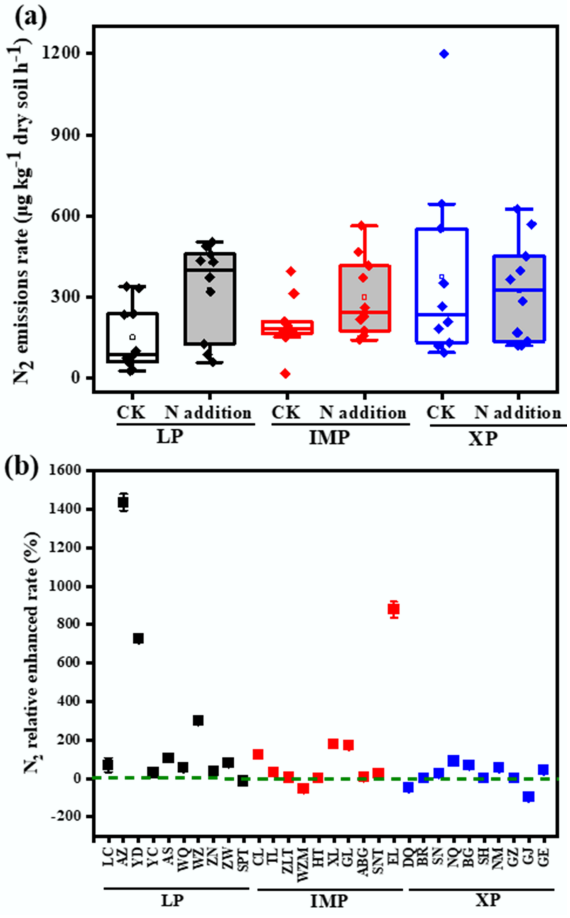

Fig. 3 N_2 emission rates of steppe soils at different sites: (**a**) without (CK), and (**b**) with N addition (N-addition), and the relative enhancement in N_2 emission rates after N addition compared to the scenario without N addition (right y axis in plane (**b**)). Loess Plateau (LP), Inner Mongolia Plateau (IMP) and Xizang Plateau (XP) steppes. The concentration of N addition is 10 kg N ha^{-1}.

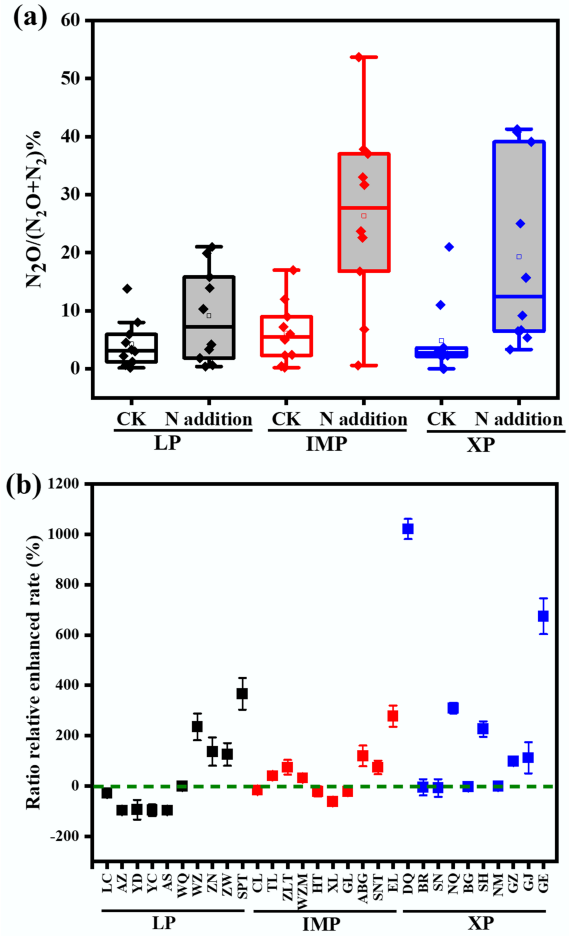

Fig. 4 Ratio of $N_2O/(N_2O + N_2)$ at different sites for the Loess Plateau (LP), Inner Mongolia Plateau (IMP), and Xizang Plateau (XP) steppes: (**a**) without (CK) and (**b**) with N addition (N-addition), and the relative enhancement in ratios after N addition compared to the scenario without N addition (right y axis in plane (**b**)). The concentration of N addition is 10 kg N ha^{-1}.

negatively correlated with MAP, moisture content, TN, NO_3^-–N, and DN. In the IMP steppe sites, N_2O emission rates were positively correlated with MAP, moisture content, TOC, TC, TN, C/N, NO_3^-–N, and N-addition; while negatively correlated with pH, bulk density, and TK. The N_2O emission rates in XP sites were correlated with all factors except for altitude, MAT, EC, TP, and NO_3^-–N. Importantly, significantly positive correlations were observed between nitrogen addition and N_2O emission rates at all sampling sites, both regionally and sub-regionally.

The correlation analysis showed that the relationships between environmental variables and N_2 emission rates varied between steppes and sites (Supplementary Table S2). Within steppes, significant correlations were observed between soil N_2 emission rates and MAP, EC, bulk density, TK, soil carbon, and soil N (not including NO_3^-–N, and DN). In the LP steppe, the N_2 emission rate correlated with MAT, MAP, pH, bulk density, OC, TC, TN, DOC, DTC, and NH_4^+. While in the IMP steppe, the N_2 emission rate correlated with EC, bulk density, TN, TP, and soil C. In the XP steppe, the N_2 emission rate was correlated with MAP, pH, TK, TN, TOC, TC, DOC, DC, NO_2^-, and NH_4^+. Nitrogen addition exhibited a significant positive correlation with the N_2 emission rate within the LP and IMP steppe but not in the XP steppes.

Table 1 The relationships between N_2O emission rate and environmental factors on a regional (all sites), and sub-regional scale (LP, IMP, and XP) evaluated by Spearman correlation analysis

	All	LP	IMP	XP
Altitude	0.007	0.218	−0.033	−0.016
MAT	−0.259**	−0.157	−0.07	−0.136
MAP	0.313**	−0.362**	0.340*	0.894**
pH	−0.450**	0.360*	−0.392**	−0.648**
Moisture	−0.001	−0.576**	0.454**	0.486**
EC	0.047	0.376**	−0.106	0.12
Bulk density	−0.231**	−0.113	−0.484**	−0.548**
TOC	0.491**	−0.269	0.601**	0.808**
TC	0.306**	−0.155	0.556**	0.818**
TN	0.512**	−0.367**	0.536**	0.900**
TP	−0.076	−0.175	0.365**	0.137
TK	0.029	0.049	−0.423**	−0.359*
C/N	−0.237**	0.481**	0.455**	−0.23
DOC	0.274**	−0.266	0.183	0.893**
DC	0.027	−0.162	−0.013	0.749**
DIC	−0.404**	0.227	−0.271	−0.335*
NO_2^-	−0.247**	−0.223	−0.033	−0.436**
NH_4^+	0.526**	0.411**	0.148	0.791**
NO_3^-	0.075	−0.397**	0.361*	0.134
DN	0.240**	−0.378**	0.361*	0.469**
N addition	0.611**	0.613**	0.522**	0.461**

Soil and environmental factors were also correlated with the $N_2O/(N_2O + N_2)$ ratio (Supplementary Table S3). Across all steppes, TOC and soil N elements (TN, NH_4^+, and DN) were positively correlated with the soil $N_2O/(N_2O + N_2)$ ratio, while MAT, pH, C/N, and DIC showed negative correlations. In the LP steppe, the $N_2O/(N_2O + N_2)$ ratio was correlated positively with altitude, pH, and C/N, but negatively with MAP, TN, and soil C (excluding DIC). The $N_2O/(N_2O + N_2)$ ratio was correlated positively with NO_3^-, but negatively correlated with pH and DIC. In the XP steppe, all variables except altitude, moisture, TP, TK, C/N, and NO_3^- were observed to be positively correlated with the $N_2O/(N_2O + N_2)$ ratio. Nitrogen addition was found to be positively correlated with the $N_2O/(N_2O + N_2)$ ratio across steppes and within steppes, similar to the N_2O emission rate.

Factors controlling denitrification potential at a regional and sub-regional scale

At the regional scale, geographical distance had a direct and significant influence on environmental variables (climate and soil physiochemical properties), while these same factors significantly influenced N_2O emission rates either directly or indirectly through their effects on soil N. The direct effect of soil N (path coefficient = 0.43) on N_2O emission rate was greater than those of soil physiochemical properties (path coefficient = −0.22) or N addition (path coefficient = 0.42) (Fig. 5a). Among the soil N components, TN showed the highest standardized coefficient (0.54) as revealed by the stepwise multiple regression analysis (Table 2), indicating that TN was a key factor explaining N_2O emission rate. At the LP sites, geographical distance had a direct and significant influence on climate, soil properties, and soil N. In addition, soil properties and soil N directly affected N_2O emission rate. The direct effect of N addition (path coefficient = 0.78) on N_2O emission rate was greater than that of soil N (path coefficient = 0.55) (Fig. 5b). Further, stepwise multiple regression analysis indicated that N addition had the highest standardized coefficient (0.89). Among environmental factors, stepwise multiple regression analysis suggested that TC had the highest standardized coefficient (Table 2). At the IMP sites, geographical distance exerted a direct and significant influence on climate and soil properties, which directly or indirectly affected N_2O emission rates. Among environmental factors, stepwise multiple regression analysis indicated that MAP had the highest standardization coefficient of 0.413 (Table 2). Moreover, the N addition (path coefficient = 0.39) also showed a direct and positively significant influence on N_2O emission rates (Fig. 5c). At the XP sites, soil N elements (path coefficient = 0.50) significantly directly affected N_2O emission rate (Fig. 5d). Among measured environmental variables, TN explained the highest standardized coefficient (0.618) by stepwise multiple regression analysis (Table 2).

In terms of the N_2O reduction rate (N_2 emission rate), PLS-PM demonstrated the optimal fit to the present data based on respective indices of model fit (GOF = 0.55, 0.66, 0.56, and 0.63). The PLS analysis revealed that N addition and environmental variables, which are embedded in different geographical regions, can influence the rate of N_2O reduction. On a regional scale, N addition (path coefficient = 0.52) had a significant direct effect on the N_2O reduction rate, while climate (total effect coefficient = 0.49) had a significant indirect effect on N_2O reduction rate through its impact on MAP. Additionally, soil nitrogen as a substrate for N_2O production exerted considerable influence on N_2O reduction rate, particularly with respect to TN (Fig. 6a). Stepwise multiple regression modeling

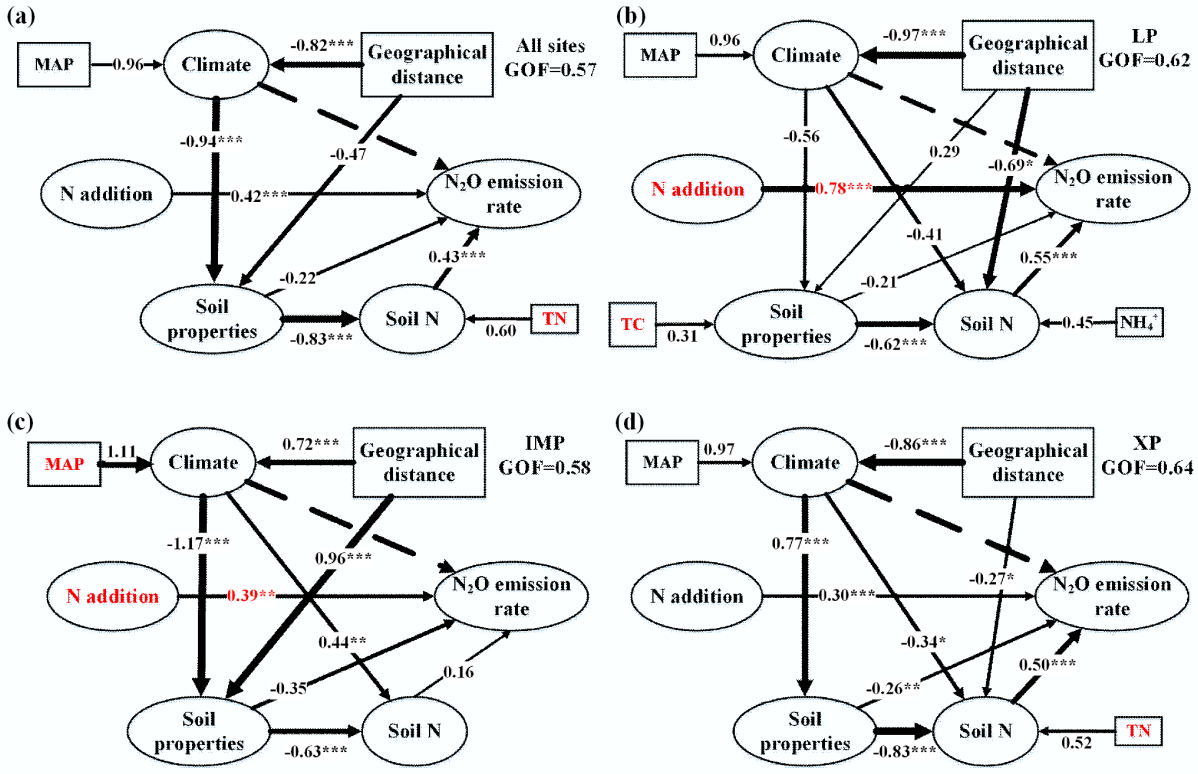

Fig. 5 Path analysis diagrams for N_2O emission rate in all sampling sites on (**a**) regional scale, and sub-regional scale (**b**) LP, (**c**) IMP, and (**d**) XP. LP, Loess Plateau; IMP, Inner Mongolia Plateau; XP, Xizang Plateau; TN, total nitrogen; MAP, mean annual precipitation; TOC, total organic carbon; NH_4^+- NH_4^+–N. Standardized coefficients are shown in Supplementary Fig. S1. Full lines and broken lines indicate that the path coefficients between latent variables are significant and not significant, respectively.

Table 2 The roles of all factors (including geographical distance, environmental variables, and N-addition) on the ratio of N_2O emission rate evaluated by stepwise multiple regression modeling on a regional (all regions), and sub-regional scale (LP, IMP, and XP)

Sites	Explanatory variable	Standardization coefficient	*p*	Full model (Adj. R^2)
All	TN	0.538	0.000	0.81
	N addition	0.373	0.000	
	Geographical distance	0.207	0.000	
	MAP	0.208	0.001	
LP	N addition	0.894	0.000	0.71
	TC	0.55	0.000	
	NO_3^-–N	−0.307	0.002	
	NH_4^+–N	0.202	0.045	
IMP	MAP	0.413	0.000	0.59
	N addition	0.366	0.001	
	TP	−0.385	0.008	
XP	TN	0.618	0.000	0.62
	N addition	0.268	0.000	
	MAP	0.186	0.029	

analysis revealed that TN (standardization coefficient = 0.49) was the most dominant factor affecting N_2O reduction rate (Supplementary Table S4). At the LP sites, N addition has a significant positive effect on soil N_2O reduction rate (Fig. 6b). Stepwise multiple regression analysis revealed that MAP (−0.49), and MAT (0.34) were key factors in explaining the N_2O reduction rate among environmental factors (Supplementary Table S4). At the IMP sites, soil physicochemical properties (path coefficient = 0.44) significantly influenced the N_2O reduction rate, followed by N addition, and soil N (Fig. 6c). Stepwise multiple regression analysis indicated that TC (0.70) and pH (0.80) dominated soil N_2O reduction rate among the soil physicochemical properties (Supplementary Table S4). At the XP sites, the contribution of N addition to N_2O reduction was relatively slight (Fig. 6d), while soil properties showed a significant directly or indirectly influence on N_2O reduction rate. And MAP showed the highest explained standardized coefficient (0.836) in the stepwise multiple regression analysis (Supplementary Table S4).

Similarly, PLS-PM analysis indicated that N addition and soil N had a significant influence on $N_2O/(N_2O + N_2)$ rate ratio (Fig. 7a), and stepwise multiple regression analysis showed that TN (0.61) was the environmental factor of the $N_2O/(N_2O + N_2)$ rate ratio on a regional scale (Supplementary Table S5). At the LP sites, geographical distance influenced $N_2O/(N_2O + N_2)$ rate ratio indirectly by its effect on soil properties and soil N (Fig. 7b), soil nitrogen, as a substrate (path coefficient = −0.21) and nitrogen addition (path coefficient = 0.21) directly but not significantly affected the $N_2O/(N_2O + N_2)$ rate ratio. Among environmental variables, TN (−0.50) dominated $N_2O/(N_2O + N_2)$ rate ratio explained by stepwise multiple regression analysis (Supplementary Table S5). At the IMP sites, soil properties influenced $N_2O/(N_2O + N_2)$ rate ratio, directly or indirectly by their effect on soil N, and N addition (path coefficient = 0.46) significantly positively influenced $N_2O/(N_2O + N_2)$ rate ratio directly (Fig. 7c). Further stepwise multiple regression analysis showed that pH (−1.05) was the most dominant factor of $N_2O/(N_2O + N_2)$ rate ratio among environmental factors (Supplementary Table S5). At the XP sites, soil properties (path coefficient = 0.61), and N addition (path coefficient = 0.46) have significant effects on $N_2O/(N_2O + N_2)$ rate ratio, directly or indirectly (Fig. 7d), and stepwise multiple regression analysis explained that N addition (0.48), and TC (0.46) had the highest standardized coefficient (Supplementary Table S5), indicating that TC dominated $N_2O/(N_2O + N_2)$ rate ratio among the environmental factors.

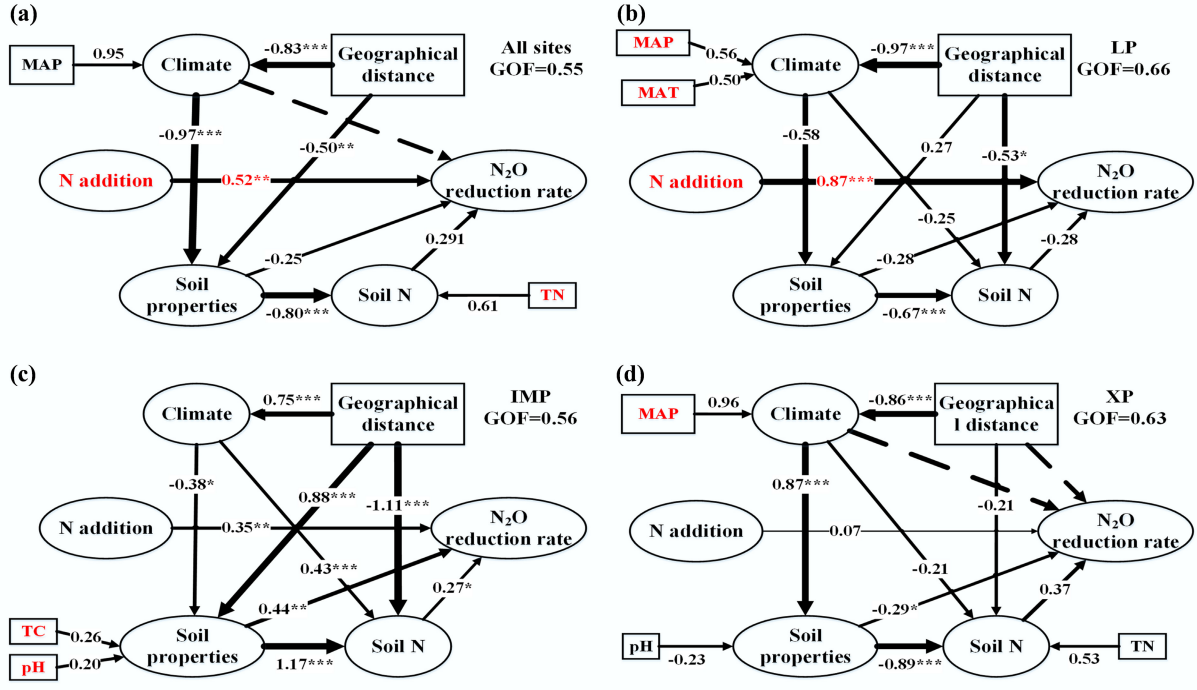

Fig. 6 Path analysis diagrams for N_2O reduction rate in all sampling sites on **(a)** regional scale, and sub-regional scale (**b**) LP, (**c**) IMP, and (**d**) XP. LP, Loess Plateau; IMP, Inner Mongolia Plateau; XP, Xizang Plateau; TN, total nitrogen; MAP, mean annual precipitation; MAT, mean annual temperature; TOC, total organic carbon; TC, total carbon. Standardized coefficient is showed in Supplementary Fig. S2. Full lines and broken lines indicate that the path coefficients between latent variables are significant, and not significant, respectively.

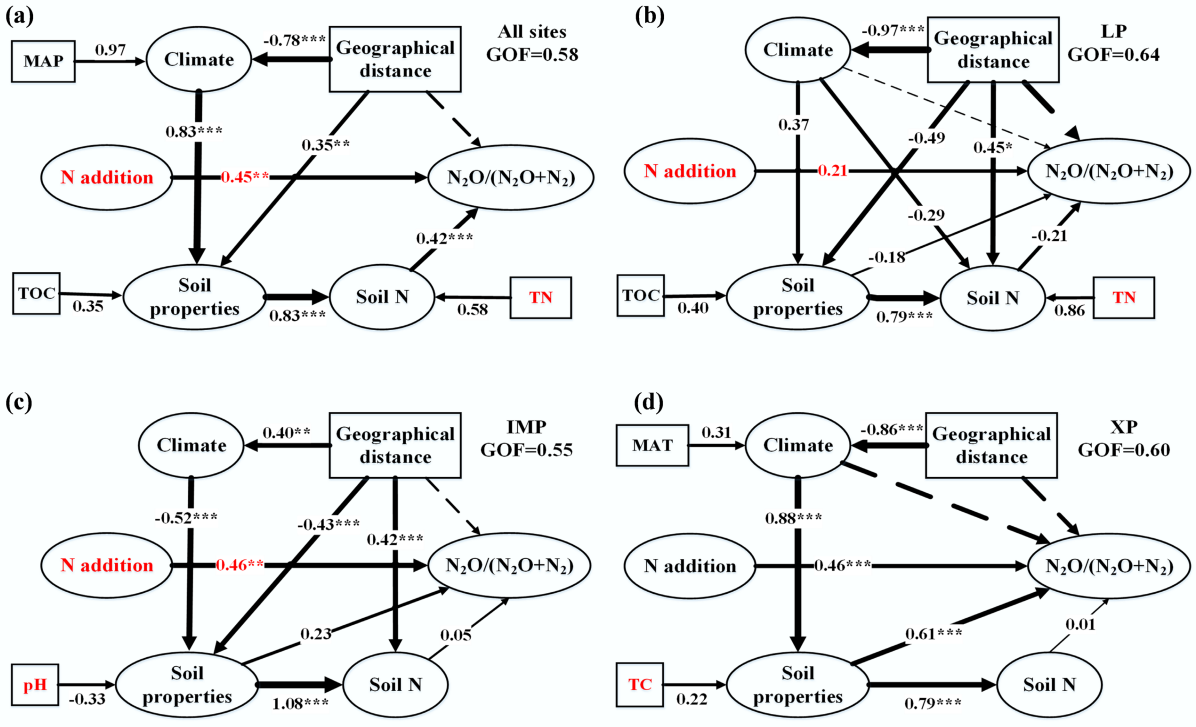

Fig. 7 Path analysis diagrams for $N_2O/(N_2O + N_2)$ rate ratio in all sampling sites on (**a**) regional scale, and sub-regional scale (**b**) LP, (**c**) IMP, and (**d**) XP. LP, Loess Plateau; IMP, Inner Mongolia Plateau; XP, Xizang Plateau; TN, total nitrogen; MAP, mean annual precipitation; TOC, total organic carbon; DN, Dissolved nitrogen; MAT, mean annual temperature. Standardized coefficient is shown in Supplementary Fig. S3. Full lines and broken lines indicate that the path coefficients between latent variables are significant, and not significant, respectively.

Discussion

In this study, the pathways and key determinants governing the denitrification potential variation across different sub-regions of the Chinese grassland biome over larger spatial scales have been uncovered. The present findings indicate that environmental factors controlling denitrification potential exhibit scale-dependent characteristics, and the effects were mainly realized through their influences on soil N elements, and/or by affecting soil physicochemical properties.

PLS modeling revealed that nitrogen (N) addition exerts a strong, scale-independent influence on denitrification rates across grassland ecosystems. This contrasts with patterns in forests and wetlands: forests experience high denitrification potential from elevated N deposition and persistent moisture, yet soil acidification inhibits sensitive denitrifiers and limits N_2O reduction[29]. Wetlands, conversely, are primarily controlled by total organic carbon (TOC)[30]. In this study, the presence of nitrate-N, as a direct substrate for denitrification, can directly impact the production and reduction of soil N_2O, thus effectively regulating soil N_2O emissions[13]. Prior studies report linear or exponential increases in N_2O emissions with increasing N addition in temperate grasslands[31,32]. However, this relationship varies by ecosystem. Specifically, alpine grasslands exhibit a saturating response (initial increase followed by stabilization) to increasing N inputs[33]. Another possible reason could be its influence on microbial communities. N addition could induce shifts in microbial community composition and activities involved in denitrification, ultimately fostering an increase in denitrifier abundance, thereby intensifying soil N_2O emissions[34,35]. Additionally, the enzyme activities associated with denitrification, and the abundance of denitrification functional genes also demonstrate a significant increase under nitrogen-enriched conditions, consequently enhancing the potential denitrification rate[36,37].

While the denitrification potential exhibited an association with soil nitrogen addition at both the regional and sub-regional scales, scale-dependent patterns were also discerned in terms of the influence of key environmental drivers on denitrification potential. At the regional scale, total nitrogen (TN) emerged as the primary determinant governing the denitrification rate. The impact of TN content on denitrification potential is multifaceted: firstly, nitrogen functions as the substrate for soil denitrification, directly impacting soil N_2O emission[38]. Secondly, elevated soil nitrogen content can directly stimulate the growth and proliferation of soil microorganisms[39]. Furthermore, it can serve as a nutrient source for surface vegetation. Flourishing vegetation, characterized by extensive exudates from well-developed roots, fosters the multiplication and activity of soil microorganisms, including denitrifying bacteria[40,41]. Wang et al.[42] have also reported that heightened TN content can bolster the activities of the soil microbial community. In essence, the augmentation in microbial abundance and activities leads to a subsequent increase in N_2O emissions.

In the LP steppe, NH_4^+ and TC emerged as primary contributors to the N_2O emission rate, while MAT and MAP stood out as key drivers for the N_2O reduction rate. Additionally, TN was identified as the pivotal environmental variable governing the $N_2O/(N_2O + N_2)$ ratio. Soil NH_4^+ played a crucial role in N_2O emission via nitrification, particularly prevalent in drier conditions, with NH_4^+ also readily assimilated into microbial biomass, nurturing microorganisms[43]. In a temperate grassland, NH_4^+ application led to elevated N_2O fluxes, significantly amplifying soil N_2O emissions by an average of 98.2% in a meadow steppe[44]. Soil carbon (TC) served as an essential energy source for various microbial activities. Denitrifiers required

easily available C before reducing NO_3^- to N_2O[45]. Enhanced soil C availability generally correlated with increased denitrification rates across various soils[46].

In the IMP steppe, MAP assumed the role of the most influential environmental variable shaping the N_2O emission rate, while TC and pH played significant roles in the N_2O reduction rate. Notably, pH also stood out as the primary determinant of the $N_2O/(N_2O + N_2)$ ratio. Terrestrial N_2O fluxes were markedly affected by MAP, with PLS path modeling demonstrating its direct and indirect influence on N_2O emission rate through soil property effects[47]. Soil moisture, primarily governed by MAP, emerged as a key factor influencing denitrification potential[48]. MAP also affected N_2O emissions indirectly through a negative effect on soil pH[47]. Soil pH held a significant role in determining denitrification rates and N_2/N_2O emission ratios in grassland soils of Northeast China. Generally, N_2O fluxes exhibited an increase with rising soil pH in grasslands[49], while a year-long field study established a negative linear correlation between soil pH and cumulative N_2O emissions in an intensively managed temperate grassland[50]. The N_2O reductase (*nosZ*) enzyme, crucial in microbial denitrification and N_2O consumption, was notably sensitive to soil pH. A higher abundance of the *nosZ* gene was observed under relatively elevated soil pH values, leading to increased N_2O conversion to N_2 and thus mitigating N_2O emissions[51,52].

In the XP steppe, TN was the most important environmental driver explaining N_2O emission and reduction rate; TC was the key environmental driver affecting the ratio of $N_2O/(N_2O + N_2)$. Research indicates that TC plays a key role in controlling denitrification potential. Correlations were observed between daily N_2O flux rates and TC in an alpine grassland[10]. The nature and quantity of soil organic carbon likely exert strong effects on the composition and activity of soil microorganisms. Kou et al.[53] also found that TOC may influence denitrifier activity through its effects on *nirK*-type denitrifier abundance at the TP alpine steppe soils, and the denitrifier abundance directly determines the denitrification potential in the soil N-related cycles.

Conclusions

In summary, this study sheds light on the scale-dependent drivers that govern denitrification potential within Chinese grassland ecosystems. These identified environmental factors can serve as singular or limited variables for estimating denitrification potential across diverse grassland ecosystems on a larger scale. Notably, in the XP, the significance of TN and TOC as controlling factors could warrant their greater emphasis within denitrification rate prediction models. However, to enhance predictive accuracy, it is advisable to devise intricate models tailored to specific sub-regions, encompassing a broader spectrum of variables and their temporal dynamics, including factors such as precipitation and temperature. In addition, the present results provide important information for the assessment of the consequences of global changes on denitrification potential in specific ecosystems or sub-regions. For instance, within the IMP steppe, MAP emerged as the pivotal controlling variable for denitrification potential, indicating a heightened sensitivity of this sub-region to climate fluctuations. Meanwhile, TN demonstrated superior explanatory power for denitrification potential within the LP. This insight suggests that Loess Plateau soils might display heightened vulnerability to nitrogen deposition compared to other sub-regions. While this study focuses on environmental drivers, microbial functional gene dynamics were not explicitly analyzed. Future work will examine how microbial activity and functional genes shape denitrification potential in China's grassland ecosystems. Overall, this study advances our comprehension of denitrification potential prediction and the intricate interplay between global changes and N_2O emissions.

Supplementary information

It accompanies this paper at: https://doi.org/10.48130/ebp-0025-0007.

Author contributions

The authors confirm contributions to the paper as follows: study conception and design: Qin S, Yuan D; data collection, analysis and interpretation of results: He X, Yuan D; draft manuscript preparation: Yuan D, He X, Clough TJ, Hu C, Li X, Yao M. All authors reviewed the results and approved the final version of the manuscript.

Data availability

All data generated or analyzed during this study are included in this published article and its supplementary information files.

Funding

This work was supported by the Natural Science Foundation of Hebei Province (D2022503014), the Hebei Province Central Guide Local Science and Technology Development Fund Project (246Z4206G), the China Postdoctoral Science Foundation (2025M772517), the Postdoctoral Fellowship Program of CPSF (GZC20251630), and the Backbone Talent Project of the Yanzhao Golden Platform for Talent Attraction in Hebei Province (Postdoctoral Platform) (B2025005034).

Declarations

Competing interests

The authors declare that they have no conflict of interest.

Author details

[1]Key Laboratory of Soil Ecology, Center for Agricultural Resources Research, Institute of Genetic and Developmental Biology, The Chinese Academy of Sciences, 286 Huaizhong Road, Shijiazhuang, Hebei 050021, China; [2]Geographic Information Division, Guangxi Zhuang Autonomous Region Land Surveying and Mapping Institute, Nanning, Guangxi 530015, China; [3]Faculty of Agriculture & Life Sciences, Lincoln University, Lincoln 7647, New Zealand; [4]Engineering Research Center of Soil Remediation of Fujian Province University, College of Resources and Environment, Fujian Agriculture and Forestry University, Fuzhou, Fujian 350002, China

References

[1] Forster P, Storelvmo T, Armour K, Collins W, Dufresne JL, et al. 2021. The earth's energy budget, climate feedbacks, and climate sensitivity. In *Climate Change 2021: the Physical Science Basis. Contribution of Working Group I 40 to the Sixth Assessment Report of the Intergovernmental Panel on Climate Change*. UK, USA: Cambridge University Press. pp. 923–1054 doi: 10.1017/9781009157896

[2] Ravishankara AR, Daniel JS, Portmann RW. 2009. Nitrous oxide (N_2O): The dominant ozone-depleting substance emitted in the 21st century. *Science* 326:123–125

[3] Harris E, Diaz-Pines E, Stoll E, Schloter M, Schulz S, et al. 2021. Denitrifying pathways dominate nitrous oxide emissions from managed grassland during drought and rewetting. *Science Advances* 7:eabb7118

[4] Ostrom NE, Sutka R, Ostrom PH, Grandy AS, Huizinga KM, et al. 2010. Isotopologue data reveal bacterial denitrification as the primary

source of N_2O during a high flux event following cultivation of a native temperate grassland. *Soil Biology and Biochemistry* 42:499–506

[5] Kang L, Han X, Zhang Z, Sun OJ. 2007. Grassland ecosystems in China: review of current knowledge and research advancement. *Philosophical Transactions of the Royal Society B: Biological Sciences* 362:997–1008

[6] Spohn M, Bagchi S, Bakker JD, Borer ET, Carbutt C, et al. 2025. Interactive and unimodal relationships between plant biomass, abiotic factors, and plant diversity in global grasslands. *Communications Biology* 8:97

[7] Chen GX, Huang B, Xu H, Zhang Y, Huang GH, et al. 2000. Nitrous oxide emissions from terrestrial ecosystems in China. *Chemosphere-Global Change Science* 2:373–378

[8] Peng Q, Qi Y, Yin F, Guo Y, Dong Y, et al. 2024. The seasonal response of N_2O emissions to increasing precipitation and nitrogen deposition and its driving factors in temperate semi-arid grassland. *Agronomy* 14:1153

[9] Yin M, Gao X, Kuang W, Tenuta M. 2023. Soil N_2O emissions and functional genes in response to grazing grassland with livestock: a meta-analysis. *Geoderma* 436:116538

[10] Yin M, Gao X, Tenuta M, Li L, Gui D, et al. 2020. Enhancement of N_2O emissions by grazing is related to soil physicochemical characteristics rather than nitrifier and denitrifier abundances in alpine grassland. *Geoderma* 375:114511

[11] Zhang J, He P, Liu Y, Du W, Jing H, et al. 2021. Soil properties and microbial abundance explain variations in N_2O fluxes from temperate steppe soil treated with nitrogen and water in Inner Mongolia, China. *Applied Soil Ecology* 165:103984

[12] Zhong L, Zhou X, Wang Y, Li FY, Zhou S, et al. 2017. Mixed grazing and clipping is beneficial to ecosystem recovery but may increase potential N_2O emissions in a semi-arid grassland. *Soil Biology and Biochemistry* 114:42–51

[13] Pan B, Xia L, Lam SK, Wang E, Zhang Y, et al. 2022. A global synthesis of soil denitrification: Driving factors and mitigation strategies. *Agriculture, Ecosystems & Environment* 327:107850

[14] Tong Y, Dong Q, Yu Y, Cao Q, Yang X, et al. 2024. Nitrogen application increases the productivity of perennial alpine cultivated grassland by improving soil physicochemical properties and microbial community characteristics. *Plant and Soil* 505:559–579

[15] Mosier A, Schimel D, Valentine D, Bronson K, Parton W. 1991. Methane and nitrous oxide fluxes in native, fertilized and cultivated grasslands. *Nature* 350:330–332

[16] Bobbink R, Hicks K, Galloway J, Spranger T, Alkemade R, et al. 2010. Global assessment of nitrogen deposition effects on terrestrial plant diversity: a synthesis. *Ecological Applications* 20:30–59

[17] Geng F, Li K, Liu X, Gong Y, Yue P, et al. 2019. Long-term effects of N deposition on N_2O emission in an alpine grassland of Central Asia. *CATENA* 182:104100

[18] Zhang B, Yu L, Wang J, Tang H, Qu Z, et al. 2022. Effects of warming and nitrogen input on soil N_2O emission from Qinghai-Tibetan Plateau: a synthesis. *Agricultural and Forest Meteorology* 326:109167

[19] Zhang B, Zhou M, Zhu B, Xiao Q, Wang T, et al. 2021. Soil type affects not only magnitude but also thermal sensitivity of N_2O emissions in subtropical mountain area. *Science of the Total Environment* 797:149127

[20] Lu Z, Du R, Du P, Li Z, Liang Z, et al. 2015. Effect of mowing on N_2O and CH_4 fluxes emissions from the meadow-steppe grasslands of Inner Mongolia. *Frontiers of Earth Science* 9:473–486

[21] Du Y, Ke X, Li J, Wang Y, Cao G, et al. 2021. Nitrogen deposition increases global grassland N_2O emission rates steeply: a meta-analysis. *CATENA* 199:105105

[22] Wei D, Xu R, Liu Y, Wang Y, Wang Y. 2014. Three-year study of CO_2 efflux and CH_4/N_2O fluxes at an alpine steppe site on the central Tibetan Plateau and their responses to simulated N deposition. *Geoderma* 232-234:88–96

[23] Wan Z, Gu R, Ganjurjav H, Hu G, Gao Q, et al. 2024. The stability of aboveground productivity in a semiarid steppe in China is influenced by the plant community structure. *Communications Earth & Environment* 5:523

[24] Xu L, Cao H, Li C, Wang C, He N, et al. 2022. The importance of rare versus abundant phoD-harboring subcommunities in driving soil alkaline phosphatase activity and available P content in Chinese steppe ecosystems. *Soil Biology and Biochemistry* 164:108491

[25] Dorich RA, Nelson DW. 1983. Direct colorimetric measurement of ammonium in potassium chloride extracts of soils. *Soil Science Society of America Journal* 47:833–836

[26] Norman RJ, Edberg JC, Stucki JW. 1985. Determination of nitrate in soil extracts by dual-wavelength ultraviolet spectrophotometry. *Soil Science Society of America Journal* 49:1182–1185

[27] Norman RJ, Stucki JW. 1981. The determination of nitrate and nitrite in soil extracts by ultraviolet spectrophotometry. *Soil Science Society of America Journal* 45:347–353

[28] Molstad L, Dörsch P, Bakken LR. 2007. Robotized incubation system for monitoring gases (O_2, NO, N_2O N_2) in denitrifying cultures. *Journal of Microbiological Methods* 71:202–211

[29] Chen Q, Han F, Lyu M, Zeng Z, Cai Y, et al. 2025. Distinct responses of fungal and bacterial denitrification genes to seasonal changes, nitrogen deposition and precipitation reduction in subtropical forest soils. *Applied Soil Ecology* 213:106322

[30] Lun J, Zhou W, Sun M, Li N, Shi W, et al. 2024. Meta-analysis: Global patterns and drivers of denitrification, anammox and DNRA rates in wetland and marine ecosystems. *Science of the Total Environment* 954:176694

[31] Hoben JP, Gehl RJ, Millar N, Grace PR, Robertson GP. 2011. Nonlinear nitrous oxide (N_2O) response to nitrogen fertilizer in on-farm corn crops of the US Midwest. *Global Change Biology* 17:1140–1152

[32] Peng Y, Wang G, Li F, Zhou G, Yang G, et al. 2018. Soil temperature dynamics modulate N_2O flux Response to multiple nitrogen additions in an alpine steppe. *Journal of Geophysical Research: Biogeosciences* 123:3308–19

[33] Liu Y, Xu-Ri, Xu X, Wei D, Wang Y, et al. 2013. Plant and soil responses of an alpine steppe on the Tibetan Plateau to multi-level nitrogen addition. *Plant and Soil* 373:515–529

[34] Ullah S, Raza MM, Abbas T, Guan X, Zhou W, et al. 2023. Responses of soil microbial communities and enzyme activities under nitrogen addition in fluvo-aquic and black soil of North China. *Frontiers in Microbiology* 14:1249471

[35] Wang X, Feng J, Ao G, Qin W, Han M, et al. 2023. Globally nitrogen addition alters soil microbial community structure, but has minor effects on soil microbial diversity and richness. *Soil Biology and Biochemistry* 179:108982

[36] Long XE, Shen JP, Wang JT, Zhang LM, Di H, et al. 2017. Contrasting response of two grassland soils to N addition and moisture levels: N_2O emission and functional gene abundance. *Journal of Soils and Sediments* 17:384–392

[37] Wei C, Su F, Yue H, Song F, Li H. 2024. Spatial distribution characteristics of denitrification functional genes and the environmental drivers in Liaohe estuary wetland. *Environmental Science and Pollution Research* 31:1064–1078

[38] Yang Y, Liu H, Lv J. 2022. Response of N_2O emission and denitrification genes to different inorganic and organic amendments. *Scientific Reports* 12:3940

[39] Zheng S, Bian H, Quan Q, Xu L, Chen Z, et al. 2018. Effect of nitrogen and acid deposition on soil respiration in a temperate forest in China. *Geoderma* 329:82–90

[40] Araya YN, Gowing DJ, Dise N. 2013. Does soil nitrogen availability mediate the response of grassland composition to water regime? *Journal of Vegetation Science* 24:506–517

[41] She W, Bai Y, Zhang Y, Qin S, Feng W, et al. 2018. Resource availability drives responses of soil microbial communities to short-term precipitation and nitrogen addition in a desert shrubland. *Frontiers in Microbiology* 9:186

[42] Wang Z, Na R, Koziol L, Schellenberg MP, Li X, et al. 2020. Response of bacterial communities and plant-mediated soil processes to nitrogen deposition and precipitation in a desert steppe. *Plant and Soil* 448:277–297

[43] Liu X, Zhang Q, Li S, Zhang L, Ren J. 2017. Simulated NH_4^+-N deposition inhibits CH_4 uptake and promotes N_2O emission in the meadow steppe of Inner Mongolia, China. *Pedosphere* 27:306–317

[44] Jones SK, Rees RM, Skiba UM, Ball BC. 2007. Influence of organic and mineral N fertiliser on N_2O fluxes from a temperate grassland. *Agriculture, Ecosystems & Environment* 121:74–83

[45] Ye J, Mark Jensen M, Goonesekera EM, Yu R, Smets BF, et al. 2024. Denitrifying communities enriched with mixed nitrogen oxides preferentially reduce N_2O under conditions of electron competition in wastewater. *Chemical Engineering Journal* 498:155292

[46] Li Z, Tang Z, Song Z, Chen W, Tian D, et al. 2022. Variations and controlling factors of soil denitrification rate. *Global Change Biology* 28:2133–2145

[47] Yin Y, Wang Z, Tian X, Wang Y, Cong J, et al. 2022. Evaluation of variation in background nitrous oxide emissions: A new global synthesis integrating the impacts of climate, soil, and management conditions. *Global Change Biology* 28:480–492

[48] Liao J, Luo Q, Hu A, Wan W, Tian D, et al. 2022. Soil moisture–atmosphere feedback dominates land N_2O nitrification emissions and denitrification reduction. *Global Change Biology* 28:6404–6418

[49] Bleken MA, Rittl TF. 2022. Soil pH-increase strongly mitigated N_2O emissions following ploughing of grass and clover swards in autumn: a winter field study. *Science of the Total Environment* 828:154059

[50] Žurovec O, Wall DP, Brennan FP, Krol DJ, Forrestal PJ, et al. 2021. Increasing soil pH reduces fertiliser derived N_2O emissions in intensively managed temperate grassland. *Agriculture, Ecosystems & Environment* 311:107319

[51] Blum JM, Su Q, Ma Y, Valverde-Pérez B, Domingo-Félez C, et al. 2018. The pH dependency of N-converting enzymatic processes, pathways and microbes: effect on net N_2O production. *Environmental Microbiology* 20:1623–1640

[52] You L, Ros GH, Chen Y, Yang X, Cui Z, et al. 2022. Global meta-analysis of terrestrial nitrous oxide emissions and associated functional genes under nitrogen addition. *Soil Biology and Biochemistry* 165:108523

[53] Kou Y, Li C, Li J, Tu B, Wang Y, et al. 2019. Climate and soil parameters are more important than denitrifier abundances in controlling potential denitrification rates in Chinese grassland soils. *Science of the Total Environment* 669:62–69